Mathl Comput. Modelling, Vol. 11, pp. 70–74, 1988
Printed in Great Britain

0895-7177/88 $3.00 + 0.00
Pergamon Press plc

A FINITE ELEMENT MODEL FOR OCEAN ACOUSTIC PROPAGATION

Joseph E. Murphy

University of New Orleans
Department of Physics
Lakefront
New Orleans, LA 70148

Stanley A. Chin-Bing

Naval Ocean Research and
Development Activity
Numerical Modeling Division
NSTL, MS 39529-5004

Abstract. The finite element method has been applied to produce a full-wave range-dependent scalar ocean acoustic propagation model. "Full-wave" includes the continuous and discrete spectra, forward propagation, and backscatter. The model is accurate at all ranges and has been validated by comparison with a coupled-mode model solution to an Acoustical Society of America benchmark problem. Two methods, super-elements and marching frames, are suggested which will give the model long-range capability.

Keywords. Full-wave acoustic propagation; ocean acoustic modeling; range-dependent acoustic propagation.

INTRODUCTION

In 1981 a Parabolic Equation (PE) ocean acoustic modeling workshop was held to compare the accuracy of PE models on selected test problems. The consensus of this workshop was that all PE models do not give the same results, and since there did not exist a benchmark range-dependent ocean acoustic propagation model against which results could be compared, the accuracy of the various PE models could not be assessed (Davis, et al., 1982). To provide a benchmark answer, a coupled-mode model was developed (Evans, 1983). The coupled-mode model is both range-dependent and full-wave, i.e., it includes both the continuous and discrete spectra (normal modes), forward propagation, and backscatter. This represented a major step forward in ocean acoustic propagation modeling since it provided the underwater acoustic community an accurate baseline against which less accurate but faster computer models could be evaluated. However, the present PE and coupled-mode models do not include range-dependent shear waves. In many ocean regions range-dependent shear waves can effect both long- and short-range underwater acoustic transmission. This is also true in polar ocean regions where shear waves in ice can effect the underwater acoustic transmission. Time-dependent geophysics models based on the finite-difference method (Stephen, 1987) do include shear and can be used to give accurate predictions, but require a great deal of computer time for only short ranges. Indeed, computation time makes the model very short-range limited. A comparison of the capabilities and deficiencies of various types of ocean acoustic propagation models is given in Table 1.

TABLE 1. CAPABILITIES OF VARIOUS TYPES OF UNDERWATER ACOUSTIC PROPAGATION MODELS

MODEL	VARIES WITH RANGE	GOOD NEAR SOURCE	FULL WAVE	HAS SHEAR
Normal Modes*	NO	NO	NO	NO
Parabolic Equation	YES	NO	NO	NO
Fast Field Program	NO	YES	YES	YES
Finite-Difference	YES	YES	YES	YES

*Some normal mode models do have an approximation to the shear in the sub-bottom layer; and, some normal mode models can also approximate range-dependency by using an adiabatic approximation.

In this paper we present the theory and results of our full-wave range-dependent ocean acoustic propagation model based on the finite-element (FE) method (Murphy and Chin-Bing, 1986) and validated by comparison with the Acoustical Society of America (ASA) benchmark problem (Felsen, 1987).

The FE method has been applied to problems in structural mechanics and fluid dynamics with phenomenal success. However, application of the FE method to underwater acoustic propagation has been sparse (Kalinowski, 1979; Bayliss, et al., 1983; Kuo, et al., 1985; Hassenzadeh, et al., 1986). This may be due to the fact that many modes are needed (approximately 10 nodes per wavelength) which greatly increases computer storage and computation time. Hence, underwater acoustic propagation models based on the FE method are usually restricted to short ranges and low frequencies. Little has been done to alleviate either of these two problems.

We have chosen to use the FE method because it is an accurate numerical solution to the full-wave range-dependent problem at all ranges (long-range, near-range, and under the acoustic source). Moreover, it is easily extendable to include shear waves. A model based on the FE method can also be extended to three dimensions in a straightforward way. The FE model we present here is a full-wave, range-dependent two-dimensional scalar model. Shear wave capability has not yet been included. We also present some ideas on overcoming the computer storage problem and the short-range limitation.

THEORY

Starting with the equation of motion, the pressure, P, can be obtained from,

$$\rho \nabla \cdot (\rho^{-1} \nabla P) + k^2 P = 0 \quad , \qquad (1)$$

where $r \neq r_{source}$, ρ is the density, and $k = \omega / c(r)$.

Multiply Eq. (1) by a test function, V, and integrated over the element "e".

$$\int_\Omega \rho^{-1} \nabla V \cdot \nabla P \, dA - \int_\Omega \rho^{-1} k^2 V P \, dA$$

$$- \int_\Gamma \rho^{-1} V \, \partial P/\partial n \, dl = 0 \qquad (2)$$

The integrals are over the area of the element, Ω, and around the boundary, Γ, of the element. The partial derivative is with respect to the normal. Take the test function to be equal to the interpolation functions, ψ, and express the pressure within the element in the form,

$$P = \sum_{j=1}^{3} P_j \, \psi_j^{(e)} \quad . \qquad (3)$$

Then Eq. (2) becomes,

$$\sum_{j=1}^{3} \left[\int_\Omega \rho^{-1} \nabla \psi_i^{(e)} \cdot \nabla \psi_j^{(e)} \, dA \right.$$

$$\left. - \int_\Omega \rho^{-1} k^2 \psi_i^{(e)} \psi_j^{(e)} \, dA \right] P_j$$

$$- \int_\Gamma \rho^{-1} \psi_i^{(e)} \, \partial P/\partial n \, dl = 0 \quad . \qquad (4)$$

If ρ and k are treated as constants within each element, the first two integrals in Eq. (4) can be done exactly. For a triangular element,

$$\psi_i^{(e)} = (1/2A) (\alpha_i + \beta_i x + \gamma_i y) \quad , \qquad (5)$$

where A is the area of the triangular element, α_i, β_i, and γ_i are constants and functions of the coordinates (x_i, y_i) of the triangular element, and the index i goes from 1 to 3 (i.e., over the nodes located at the vertices of each triangle). The interpolation functions satisfy the conditions,

$$\psi_j (x_i, y_j) = \delta_{i,j} \qquad i,j = 1,2,3 \qquad (6)$$

$$\sum_{i=1}^{3} \psi_i = 1 \quad . \qquad (7)$$

The first and second terms in Eq. (4) are evaluated using the stiffness, K, and mass, M, integrals, respectively.

$$K \equiv \int_\Omega \nabla \psi_i^{(e)} \cdot \nabla \psi_j^{(e)} \, dA \qquad (8)$$

$$M \equiv \int_\Omega \psi_i^{(e)} \psi_j^{(e)} \, dA \qquad (9)$$

The third integral in Eq. (4) is the boundary integral. For an element in the interior of the FE mesh, this boundary integral will be exactly cancelled by a similar term from neighboring elements since $(1/\rho)\partial P/\partial n$ must be continuous.

For the case where the element has one or two of its sides on an actual boundary of the FE model, we allow three possible boundary conditions:

(1) Neumann Boundary Condition, $\partial P/\partial n = 0$. This is treated exactly in our FE model. The boundary term is zero.

(2) Dirichlet Boundary Condition, $P = 0$. This is also treated exactly. $\partial P/\partial n$ becomes unknown which can be found after the pressure has been found at all nodes.

(3) Radiating Boundary Condition. Waves should pass through the boundary without reflection. This is treated approximately by two boundary conditions – a narrow angle radiation boundary condition and a wide angle radiation boundary condition.

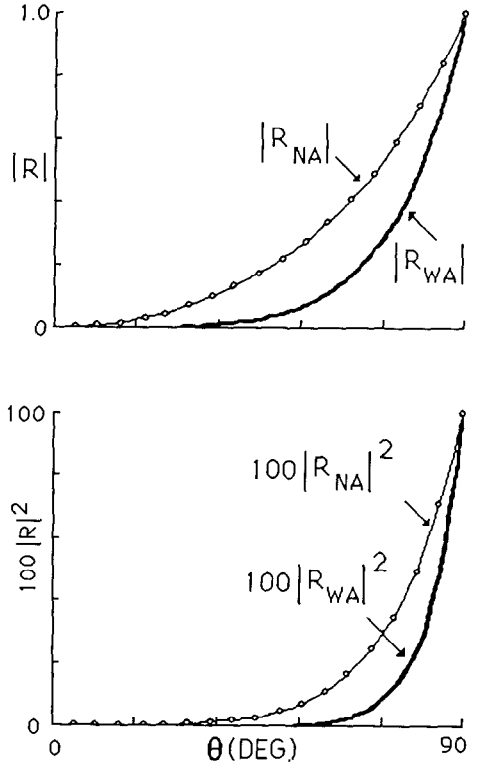

FIG.1. Comparisons of narrow angle (NA) and wide angle (WA) reflection coefficients (R) and relative intensities ($100R^2$) as a function of incident angle.

NARROW ANGLE:

$$\partial P/\partial n = i \, (\omega/c) \, P = i \, k \, P \qquad (10)$$

WIDE ANGLE:

$$\partial P/\partial n = i \, k \, [1 + (1/2k^2) \, \partial^2/\partial t^2] \, P \qquad (11)$$

The partial derivative is taken with respect to the tangent direction. A comparison that shows the advantage of the wide angle over the narrow angle boundary condition can be made using plane wave reflection coefficients. Figure 1 shows this comparison between the plane wave reflection coefficients calculated from Eqs. (10) and (11). For the same reflected intensity, the wide angle boundary condition allows a higher incident angle to be reached before the solution is seriously contaminated by artificial reflections from the computational boundary.

The equations are assembled in the usual way to produce a global stiffness matrix and global force vector (see, for example, Reddy, 1984).

RESULTS

Lloyd Mirror Effect

As a test of the accuracy of our FE model, the Lloyd mirror effect was examined. The Lloyd mirror effect, or image-interference effect, occurs in underwater acoustics when the acoustic source is near the sea surface and the sea surface is not very rough (i.e., the sea surface acts as a free pressure-release surface). Then an interference pattern in the sound field results from constructive and destructive interference between the direct and surface-reflected acoustic waves. The Lloyd mirror effect has an analytic solution (Officer, 1958) and thus was used as a baseline result against which our FE model could be compared. Figure 2 is a contour plot of constant pressure at 2 dB intervals for an upper half-space of air and a lower half-space of water with 0.5 dB per wavelength absorption. The acoustic source was placed 100 m below the surface, i.e., 100 m below the interface separating the two half-spaces. The familiar Lloyd mirror beams (Schmidt and Jensen, 1985) are quite evident.

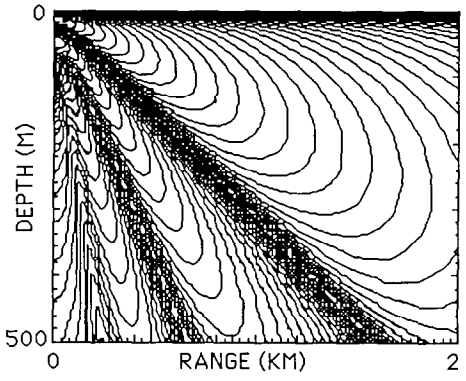

FIG. 2. Lloyd Mirror effect produced by an exact solution.

Figure 3 shows the result from our FE model applied to the same Lloyd mirror problem. Unlike the analytic solution, our model must simulate the lower half-space using a bounded medium terminating with a radiation boundary condition. The results shown in Fig. 3 were obtained using the wide-angle radiation boundary condition on the bottom and right boundaries of our model. The results from our FE model compare favorably with the analytic solution except near the radiating boundaries of the FE model. Some low grazing angle reflections are evident along the bottom and right side as can be seen by comparing Figs. 2 and 3.

A comparison of calculated transmission loss (TL), in dB., from our FE model and from the analytic solution shows that they are in complete agreement at a receiver depth of 30 m but slightly out-of-phase at a receiver depth of 150 m. This is because the wide-angle radiation condition (applied at 800 m depth) is insufficient for regions near the radiating boundaries and thus slightly effects the deeper receiver at 150 m.

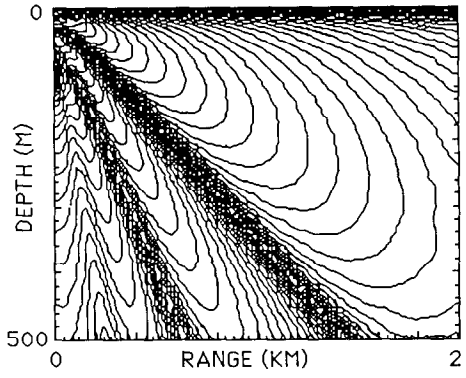

FIG. 3. Lloyd Mirror effect produced by the FE model.

ASA Benchmark Problem

In 1987 at the 113th meeting of the Acoustical Society of America (ASA), a special session was devoted to numerical solutions of benchmark problems (Felsen, 1987). One problem dealt with upslope propagation in a wedge-shaped underwater channel. A 25 Hz. CW acoustic source was placed at a depth of 100 m below the surface of the water.

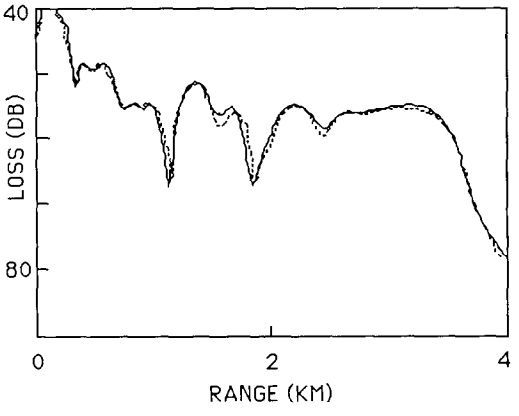

FIG. 4. Comparison of FE and coupled-mode model results for ASA benchmark problem. Solid line is FE model result and broken line is coupled-mode model result.

The ocean bottom was initially (i.e., at the source location) 200 m deep and gradually decreased in depth at a 2.86° rise until it intersected the ocean surface at a range of 4.0 km. The density of the water was 1 gm/cc and the sound speed was 1500 m/s. The wedge half-space had a density of 1.5 gm/cc, a sound speed of 1700 m/s, and an attenuation

of 0.5 dB/wavelength. A receiver was placed at a depth of 30 m and the transmission loss in dB as a function of range was computed by various numerical ocean acoustic models. A coupled-mode model (Evans, 1983) was used as the benchmark result (Jensen, 1987) against which other models were compared.

Figure 4 shows a comparison of our FE model results (solid curve) compared to the coupled-mode benchmark model results (broken curve). Both models are full-wave range-dependent models and can account for the backscatter and interference that comes from the wedge. Clearly our FE model compares favorably with the benchmark result.

FUTURE DEVELOPMENT

Radiation Boundaries

As noted in the discussion on the Lloyd mirror effect, the present radiation conditions in our FE model do not adequately handle low grazing angle reflections. This can cause errors in model predictions if the region of interest is near one of the radiating boundaries. This problem of removing unwanted boundary reflections is usually solved by adding an artificial bottom layer to the model (Lee and Botseas, 1982). This consists of placing the boundary far away from the regions of interest and adding exponentially increasing attenuation in the region just before the boundary. The boundary itself is treated as a free pressure-release surface. While this is an effective way to eliminate the unwanted reflections, applying it to the FE method would mean adding many extra elements to the model. The number of elements could be doubled resulting in a significant increase in computer memory and run time. In our FE model, unwanted boundary reflections can be eliminated without a sizable increase in elements since the wide-angle radiation condition can be applied at the boundary with just a small region of increasing attenuation preceding the boundary. Higher grazing angle radiation will be eliminated by the wide-angle radiation condition. The attenuated region will adequately dampen those low grazing angle reflections that are not eliminated by the wide-angle radiation condition.

Super-Elements

In ocean acoustics, the pressure field is not usually required at all depths and ranges but rather at only certain depths and ranges. This observation can be used to reduce the computer memory and storage needed to run a long-range acoustic propagation problem. Such a problem would normally require a large number of elements when using a FE model. However, the original number of elements (nodes) can be reduced by recursive static condensation whereby unknowns corresponding to interior nodes are eliminated (see Fig. 5).

This creation of super-elements (Axelsson, and Barker, 1984) could greatly reduce the required computer memory and storage while maintaining all modeling capability – the super-elements would be so chosen that they lay along those depths and ranges of interest. The technique is illustrated in Fig. 5 where the original number of nodes is shown in Stage 1. Stages 2 and 3 show how the interior nodes can be eliminated, i.e., they have now been condensed into the super-elements shown in Stage 3.

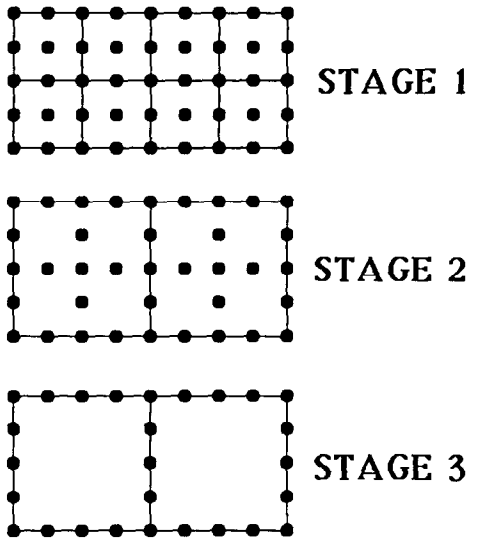

FIG. 5. Illustration of how successive application of super-elements may be used to reduce a full finite-element problem (Stage 1) to a reduced problem (Stage 3).

Marching Frames

For extremely long-range ocean propagation problems, even super-elements will not likely be sufficient to keep the amount of required computer memory and storage tractable. For such cases, we introduce the concept of "marching frames." This technique is illustrated in Fig. 6 for a long-range range-dependent ocean.

A long-range range-dependent ocean region would be

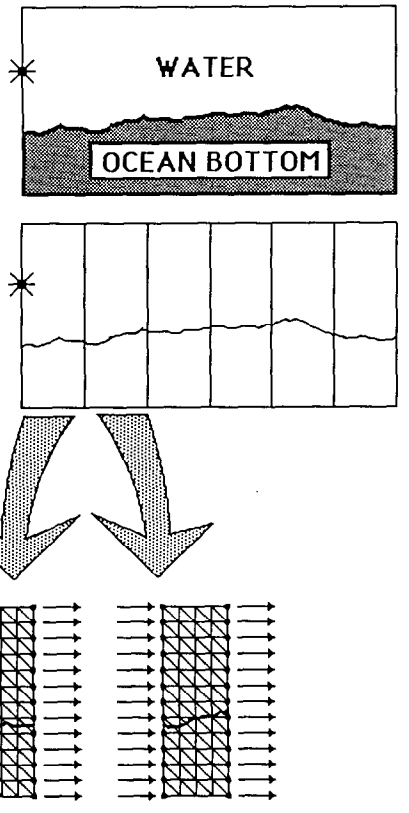

FIG 6. Illustration of how the concept of "marching frames" could be used to obtain long-range acoustic propagation in a range-dependent ocean.

divided into smaller regions (frames). The FE model would be used in the first frame to produce the pressure field at all the nodes in that frame. The pressures at the right boundary nodes would be then be used as inputs to the second frame and the FE model again run to produce the field at all node points within the second frame. This process would be sequentially repeated until the entire range was covered. In this way, the pressure field could be found at each required range and depth point as the solution (frames) marched outward in range. The concept is analogous to the range step marching solution of the parabolic equation models. Note that within each frame, the calculated fields would be precise in that they would include the forward propagation, backscatter, continuous and discrete spectra, shear (if it were included in the FE model), and range dependency. However, backscatter that could occur from some long-range topography, for example Frame 10, would not be accounted for in Frame 1. This is usually not a serious problem in long-range ocean acoustic propagation. If a far-range feature did have a large backscatter effect on a preceding frame(s), the size of the preceding frames could be adjusted so that the backscatter would be included. Since a radiating boundary condition would be used at the right boundary of each frame, the problem of unwanted boundary reflections would have to be considered. This problem could be overcome by using those pressures calculated at a few nodes to the left of each frame's right boundary (rather than the pressures on the frame's right boundary) as the inputs to the next frame. Thus, the inputs to each frame would be from a region in the previous frame where unwanted boundary reflections did not reach.

CONCLUDING REMARKS

First, we have presented an ocean acoustic propagation model that includes:

(1) the continuous spectra,
(2) the discrete spectra,
(3) forward propagation,
(4) backscatter,
(5) range-dependency.

The model is presently a scalar model, i.e., it does not include shear waves. The inclusion of range-dependent shear is the next step in our model's evolution.

Second, we have validated the accuracy of our FE model by comparing it to the coupled-mode model results from the ASA benchmark problem.

Finally, we have presented two approaches (super-elements and marching frames) to overcome the usual FE models' requirement of large computer storage. Thus, the possibility of achieving long-range ocean acoustic simulation capability using a FE approach seems feasible.

ACKNOWLEDGMENTS

This work was supported by the Office of Naval Research (ONR) and the Naval Ocean Research and Development Activity. JEM was supported by ONR ASEE Summer Faculty Research Program grants.

REFERENCES

Axelsson, O., and V. A. Barker, (1984). Finite Element Solution of Boundary Value Problems. Academic Press, New York, pp. 296-304.

Bayliss, A., C. I. Goldstein, and E. Turkel (1983). An iterative method for the Helmholtz equation. J. Comp. Phys., 49, 443-457.

Davis, J. A., D. White, and R. C. Cavanagh (1982). NORDA Parabolic Equation Workshop, 31 March - 3 April 1981. Technical Note 143, Naval Ocean Research and Development Activity, NSTL, MS.

Evans, R. B. (1983). A coupled mode solution for acoustic propagation in a waveguide with stepwise depth variations of a penetrable bottom. J. Acoust. Soc. Am., 74, 188-194.

Felsen, L. B. (1987). Numerical solutions of two benchmark problems. J. Acoust. Soc. Am. Suppl. 1, 81, S39.

Hassenzadeh, S., Y. Teng, and J. T. Kuo (1986). Finite-element analysis of marine sediment acoustics. J. Acoust. Soc. Am. Suppl. 1, 80, S64.

Jensen, F. B. (1987). Coupled mode and parabolic equation solutions. J. Acoust. Soc. Am. Suppl. 1, 81, S40.

Kalinowski, A. J. (1979). Finite element method. In J. A. DeSanto (Ed.), Ocean Acoustics, Springer-Verlag, New York, pp. 142-154.

Kuo, J. T., Y. C. Teng, P. Pecholcs, and J. Blair (1985). A note on the influence of the elasticity on wave propagation in an acoustic/elastic coupled medium. In M. H. Schultz and D. Lee (Eds.), Computational Ocean Acoustics, Pergamon Press, New York, pp. 887-896.

Lee, D. and G. Botseas (1982). IFD: An Implicit Finite-Difference Computer Model for Solving the Parabolic Equation. Technical Report 6659, Naval Underwater Systems Center, New London, Connecticut, pp. 3-11 through 3-15, and p. A-17.

Murphy, J. E., and S. A. Chin-Bing (1987). The finite element method applied to ocean acoustic propagation. J. Acoust. Soc. Am. Suppl. 1, 81, S9.

Officer, C. B.(1958). Introduction to the Theory of Sound Transmission, McGraw-Hill, New York, pp. 110-115.

Reddy, J. N. (1984). An Introduction to the Finite Element Method. McGraw-Hill, New York.

Schmidt, H. and F. B. Jensen (1985). Efficient numerical solution technique for wave propagation in horizontally stratified environments. In M. H. Schultz and D. Lee (Eds.), Computational Ocean Acoustics, Pergamon Press, New York, pp. 706-708.

Stephen, R. A. (1987). Finite difference solutions. J. Acoust. Soc. Am. Suppl. 1, 81, S40.